Clinical Radiology 74 (2019) 814.e21–814.e28

Contents lists available at ScienceDirect

Clinical Radiology

journal homepage: www.clinicalradiologyonline.net

Role of intravoxel incoherent motion MRI in preoperative evaluation of DNA mismatch repair status in rectal cancers

C. Yan [a,1], S. Liu [a,1], X. Pan [a], G. Chen [b], W. Ge [b], W. Guan [c], S. Liu [a], M. Li [a], J. He [a,*], Z. Zhou [a,*]

[a] *Department of Radiology, Nanjing Drum Tower Hospital, The Affiliated Hospital of Nanjing University Medical School, Nanjing, 210008, China*
[b] *Department of Gastrointestinal Surgery, Nanjing Drum Tower Hospital, The Affiliated Hospital of Nanjing University Medical School, Nanjing, 210008, China*
[c] *Department of Pathology, Nanjing Drum Tower Hospital, The Affiliated Hospital of Nanjing University Medical School, Nanjing, 210008, China*

ARTICLE INFORMATION

Article history:
Received 20 June 2018
Accepted 10 July 2019

AIM: To explore the role of intravoxel incoherent motion (IVIM) magnetic resonance imaging (MRI) in evaluating DNA mismatch repair (MMR) status of rectal cancers preoperatively.

MATERIALS AND METHODS: Seventy-six patients with a diagnosis of rectal cancer confirmed at endoscopic biopsy were enrolled prospectively and underwent IVIM MRI before surgery.

RESULTS: The perfusion fraction (f) values of MMR proteins (MMRP) positive rectal cancers were significantly higher than negative cancers. The f values could differentiate MMRP positive rectal cancers from negative cancers with an area under the curve (AUC) of 0.695. The vascular endothelial growth factor (VEGF) and vascular endothelial growth factor receptor 2 (VEGFR2) expression rates of positive MMRP rectal cancers were significantly higher than negative cancers.

CONCLUSION: This pilot study indicated that the f value derived from IVIM MRI differed significantly between rectal cancers with different MMRP expression levels, which might be involved with different VEGF and VEGFR2 expression rates.

Introduction

Colorectal cancer (CRC) is the fourth most common cause of cancer-related death worldwide, and approximately one-third of CRCs occur in the rectum.[1,2] DNA mismatch repair (MMR) status is one of the most well-established predictive and prognostic biomarkers in CRCs, and MMR gene abnormalities are detected in approximately 15% of all CRCs.[3,4] MMR status was traditionally determined through

* Guarantor and correspondent: Zhengyang Zhou and Jian He, Department of Radiology, Nanjing Drum Tower Hospital, The Affiliated Hospital of Nanjing University Medical School, 321 Zhongshan Road, Nanjing 210008, China. Tel.: +862583597518; Fax. +86253317761.
E-mail addresses: hjxueren@126.com (Z. He), zyzhou@nju.edu.cn (Z. Zhou).
[1] Joint first authors.

https://doi.org/10.1016/j.crad.2019.07.004
0009-9260/

immunohistochemical (IHC) staining for the four mismatch repair proteins (MMRP), MLH1, MSH2, MSH6, and PMS2, or by microsatellite instability (MSI) testing in resected specimens[5]; however, neoadjuvant chemoradiotherapy is becoming more widely used in CRC patients, which has deleterious effects on MSH6 staining,[6–8] and even resected materials may not contain any residual tumour tissues.[9] Hence, it is necessary to acquire the MMR status before neoadjuvant treatment of rectal cancers. In addition, accurate pre-treatment information of MMR status would facilitate personalised medicine for those patients. For instance, if Lynch syndrome is suspected, an extended resection should be considered to prevent metachronous cancer formation (endometrial or ovarian cancer, etc.).[10] Therefore, biopsy assessment is extensive before any treatment. Several studies have demonstrated that biopsy samples are as good as or even superior to the resected materials in evaluating MMRP expression levels[11–13]; however, it was reported that the smaller, more limited size of biopsy tissues may potentially increase the false-negative rate of MMR IHC staining.[10]

Magnetic resonance imaging (MRI) is routinely performed in the preoperative assessment of rectal cancers,[14–17] where T2-weighted (T2W) and diffusion-weighted imaging (DWI) play an important role. In particular, DWI could quantify water molecular diffusion non-invasively in terms of apparent diffusion coefficient (ADC) values.[18] Previous studies have investigated the correlations between ADC values and histopathological features of rectal cancers, yet with inconsistent findings. For instance, Sun *et al.* reported different ADC values of rectal cancers at different T stages,[19] while others detected no significant findings.[20,21] Curvo-Semedo *et al.* reported different mean tumour ADCs between rectal cancers with and without lymph node metastasis or between mesorectal fascia-free and mesorectal fascia-invaded tumours,[20] while Akashi *et al.* reported no significant findings.[21] One possible explanation for those contradictory conclusions may be that the ADC value of rectal cancers was influenced by both thermally driven motion (pure diffusion) and microcirculation blood perfusion.[18]

Intravoxel incoherent motion (IVIM) MRI, which separates pure diffusion from perfusion-related motion of water molecules,[22] provides values for the pure diffusion coefficient (D), perfusion-related incoherent microcirculation (D*), and perfusion fraction (f). Currently, there is growing interest in applying IVIM MRI in the assessment of rectal cancer response to chemotherapy and lymph node metastasis.[23–28] Recently, Surov *et al.* documented the correlations between IVIM parameters and histopathological indexes including cell count, nucleic areas, proliferation index Ki-67, and microvessel density of rectal cancers.[29] A previous study demonstrated that the f value derived from IVIM MRI might be useful to predict lymphovascular invasion status of rectal cancers preoperatively;[30] however, the association between IVIM parameters and gene and molecular expression of rectal cancers has not been reported. Therefore the aim of the present study was to explore the role of IVIM MRI to preoperatively evaluate the MMR status of rectal cancers.

Materials and methods

Participants

This prospective study was approved by the ethics committee of the Institutional Review Board of Nanjing Drum Tower Hospital, and written informed consent was obtained from all the patients. All experiments were performed in accordance with relevant guidelines and regulations. From July 2015 to February 2017, a total of 163 patients with a suspected diagnosis of rectal cancer presented to the hospital. The inclusion criteria were patients (1) with a diagnosis of rectal cancer confirmed by endoscopic biopsy; (2) willing to undergo MRI examination for preoperative assessment; and (3) absence of any absolute contraindications to MRI examination, such as cardiac pacemaker or defibrillator, aneurysm clip, nerve stimulator, insulin pump, cochlear implant, severe hepatic and renal dysfunction, or drug allergy. The exclusion criteria were patients (1) with any local or systemic treatment before MRI examination or surgery (n=32); (2) without postoperative histopathological examination due to palliative or abandoned surgery (n=9); (3) tumour with a maximum diameter <5 mm, which was insufficient to contain a region of interest (ROI) for image analysis (n=16); (4) poor-quality MRI images due to motion or magnetic susceptibility artefacts (n=6; Fig 1). Finally, 76 patients (43 men, 33 women; mean age 60.8±9.3 years; age range, 43–85 years) were prospectively included in this study (Table 1).

MRI examination

MRI was performed after the patients fasted for 6–8 hours to empty their gastrointestinal tracts. One hundred and thirty-nine grams of polyethylene glycol electrolyte powder compound (139 g in 2000 ml water; Jiangxi Hygecon Drug Research Institute Company Limited, Shangrao, China) was taken orally 5 hours before the MRI examination for those patients able to take laxatives (n=51), and the administration of an enema was undertaken 2 hours prior to the MRI examination for those patients with bowel obstruction (n=25), for purpose of reducing artefacts induced by gas and faeces within the rectum.

All patients were scanned in the head-first supine position using a 3 T MRI system (Ingenia, Philips Medical Systems, Best, the Netherlands) with a dStream Torso coil. The field of view was set from the superior border of ilium to the lower margin of the pubic bone. MRI sequences included sagittal T2-weighted imaging (repetition time [TR]= 1,700–5,000 ms, echo time (TE)=100 ms, matrix size=480×354, field of view=24×24 cm^2, section thickness=4 mm, intersection gap=1 mm, and number of signals averaged (NSA)=2), axial T2-weighted imaging (TR=1,700–5,000 ms, TE=100 ms, matrix size=480×300, field of view=24×15.9 cm^2, section thickness=4 mm,

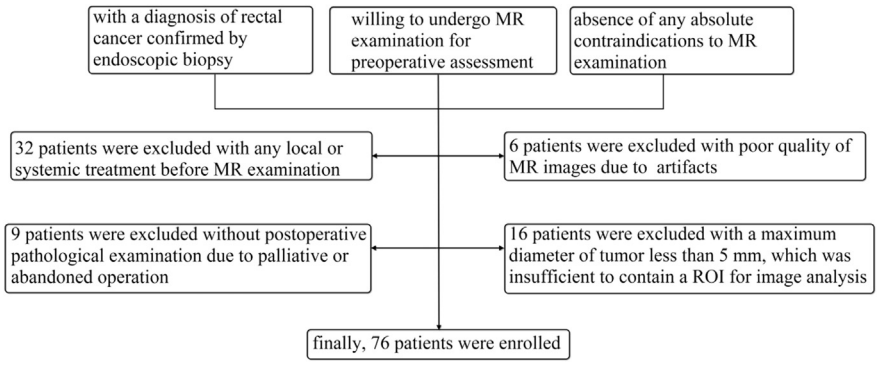

Figure 1 Inclusion and exclusion flowchart of this study.

intersection gap=1 mm, and NSA=2), coronal T2-weighted imaging (TR=3,000 ms, TE=75 ms, matrix size=300×189, field of view=18×12.7 cm^2, section thickness=3 mm, intersection gap=1 mm, and NSA=2), and axial contrast-enhanced imaging (TR=3.1 ms, TE=1.48 ms, matrix size=256×194, field of view=38.2×29.2 cm^2, section thickness=1.5 mm, intersection gap=0 mm, and NSA=1). The axial IVIM sequence used 12 b-values (0, 25, 50, 75, 100, 150, 200, 400, 600, 800, 1,000, 1,200 s/mm^2) with a single-shot echo-planar imaging sequence (TR=6,000 ms, TE=59 ms, matrix size=80×143, field of view=30×15.9 cm^2, section thickness=4 mm, intersection gap=1 mm, and NSA=2). The total scanning time was approximately 20 minutes. The mean interval (mean values ± standard deviation) between MRI examination and surgery was 3±0.4 days (range, 1–6 days).

Table 1
Clinicopathological characteristics of 76 patients with rectal cancers.

Characteristic	Group	*n*	Percentage (%)
Age	≥ 60 years	46	60.5
	< 60 years	30	39.5
Gender	Male	43	56.6
	Female	33	43.4
Carcinoembryonic antigen	≥ 5 ng/ml	42	55.3
	< 5 ng/ml	34	44.7
Cancer antigen 19-9	≥ 37 u/ml	23	30.3
	< 37 u/ml	53	69.7
Pathological type	Adenocarcinoma	76	100
	Mucinous adenocarcinoma	0	0
Differentiation degree	Poor	2	2.6
	Poor-moderate	10	13.2
	Moderate	58	76.3
	Moderate-well	3	3.9
	Well	3	3.9
pT	T1	4	5.3
	T2	20	26.3
	T3	52	68.4
	T4	0	0
pN	N0	32	42.1
	N1	20	26.3
	N2	24	31.6
cM	M0	72	94.7
	M1	4	5.3
Overall stage	I	11	14.5
	II	20	26.3
	III	40	52.6
	IV	5	6.6

Image analyses

All MRI images were analysed by two radiologists (C.C.Y., and S.L.L., with 7 and 2 years of experience in gastrointestinal radiology, respectively) independently, who were blinded to the endoscopic and surgical pathological findings.

The IVIM data were evaluated using the DWI-Tool developed by Philips (IDL 6.3, ITT Visual Information Solutions, Boulder, CO, USA) to generate ADC, D, f, and D* maps, which used the robust nonlinear least-squares curve fittings based on the Levenberg–Marquardt algorithm. ADC values were obtained with 12 b-values from mono-exponential fit to the equation: $S=S_0\times\exp(-b\times ADC)$, in which S_0 is the signal without diffusion weighting and S is the signal with diffusion weighting. A bi-exponential model was applied to calculate D, f, and D* values with the following function: $SI/SI_0=(1-f)\times\exp(-b\times D) + f\times\exp(-b\times D^*)$, where SI represents the signal intensity at a certain b-value and SI_0 represents the signal intensity at a b-value of 0 s/mm^2.

Compared with normal rectum wall, the rectal cancer appeared as a mass with iso- or slightly hyperintensity on T2-weighted images, hyperintensity on IVIM MRI images and isointensity on T1-weighted images, with remarkable enhancement on contrast enhanced sequence. By reference to other MRI sequences, three axial IVIM images (b=1,000 s/mm^2) which displayed the largest area of the tumour were selected. The ROIs were manually drawn within the solid part of the mass as large as possible (mean: 63.6±4.5 mm^2; range, 48.5–81.8 mm^2) carefully excluding necrotic and cystic areas as well as haemorrhage. The ROIs were automatically copied to the ADC, D, f, and D* maps and the mean value of each ROI were acquired. The average value of the three sections and mean values of the two radiologists were calculated as the final results for statistical analyses (Figs 2 and 3).

Surgical pathological analysis

Forty-five patients underwent anterior resection, while 22 patients received abdominoperineal resection, and nine patients underwent Hartmann resection. Each patient had

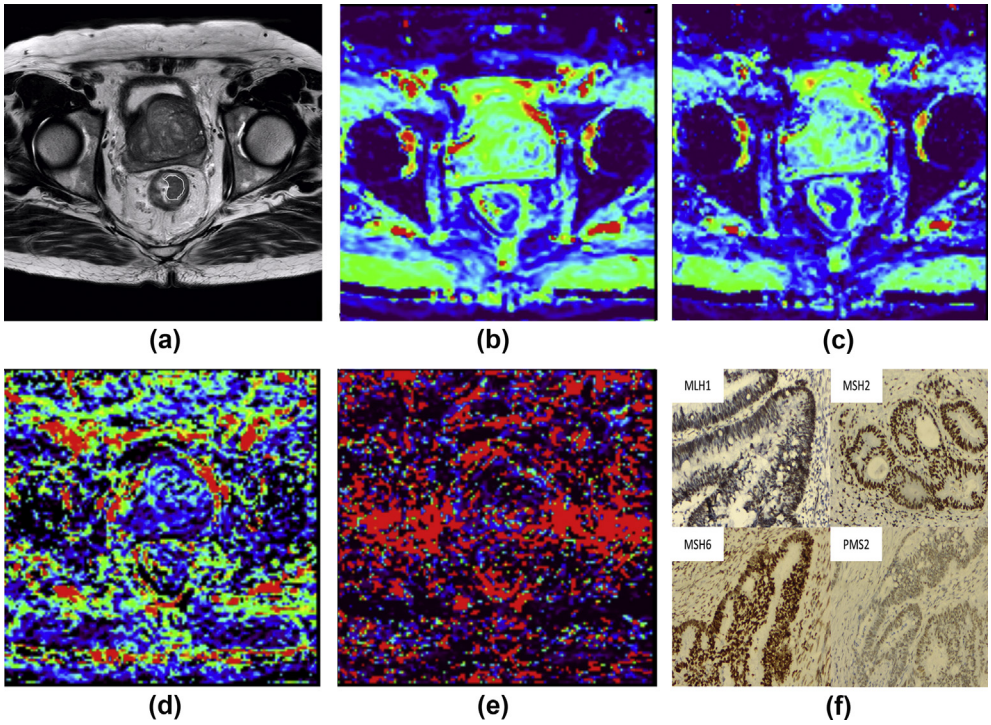

Figure 2 A 77-year-old man with rectal cancer histopathologically diagnosed as stage T2 N1c cM0. (a) Axial T2-weighted MRI image shows a mass in the rectal wall. (b) The corresponding ADC, (c) pure diffusion coefficient D, (d) perfusion related fraction f; and (e) pseudo-diffusion coefficient D* maps show that this lesion has an ADC value of 0.918×10^{-3} mm^2/s, a D value of 0.710×10^{-3} mm^2/s, a f value of 0.186 and a D* value of 17.170×10^{-3} mm^2/s, respectively. (f) Photomicrograph (Immunohistochemical staining, 200×) shows an adenocarcinoma with high expression levels of MMRP.

one lesion identified. Histopathological analysis of the resected specimens was performed by the pathologist (W.Y.G., with 7 years of experience in gastrointestinal pathology), who was blinded to the MRI findings.

A series of formalin-fixed, paraffin-embedded tissues from those patients enrolled in the study were analysed using immunohistochemistry for the four MMRP (MLH1, MSH2, MSH6, and PMS2), Ki67, epidermal growth factor receptor (EGFR), VEGF, and VEGFR2 expression. After hybridisation and antigen retrieval, the sections were stained with mouse anti-human MLH-1 antibody (clone ES05; Leica, Newcastle, UK), mouse anti-human MSH-2 antibody (clone 25D12; GeneTex, Irvine, CA, USA), rabbit anti-human MSH-6 antibody (clone EP49; Epitomics, Burlingame, CA, USA), rabbit anti-human PMS2 antibody (clone EP51; Epitomics, Burlingame, CA, USA), monoclonal mouse anti-human Ki-67 antibody (clone UMAB107; OriGene, Rockwell, MD, USA), monoclonal mouse anti-human EGFR antibody (clone UMAB96; OriGene, Rockwell, MD, USA), polyclonal rabbit anti-human VEGF antibody (Dako, Copenhagen, Denmark), and polyclonal rabbit anti-human VEGFR2 antibody (Spring Bioscience, Pleasanton, CA, USA) at 37°C for 60 minutes. Then the sections were visualised using EnVision FLEX, High pH (K8001, Dako, Copenhagen, Denmark) 3, 30-diaminobenzidine (DAB) and subsequently counterstained with haematoxylin.

In the present study, MMRP were described as negative for absent or $<10\%$ nuclear staining, and positive for $\geq10\%$ nuclear staining.[31,32] Low proliferation index was considered as Ki-67 $\leq40\%$, and high proliferation index was regarded as Ki-67 $>40\%$.[33] EGFR, VEGF, and VEGFR2 expression was determined by assessing the percentage of tumour cells with membrane staining and staining intensity: 0, no staining; I, weak staining and/or staining in $<10\%$ of tumour cells; II, distinct staining and/or staining in 10–50% of cells; III, strong staining and/or staining in $>50\%$ of cells.

MSI was analysed using polymerase chain reaction (PCR) amplification of microsatellite foci, in which the reagents were from Shanghai Yuanqi Bio-Pharmaceutical Company, China. Samples with instability in two or more of these markers were defined as MSI-H, whereas those with one unstable marker were designated as MSI-L. Samples with no detectable alterations were defined as MSS.

When grouping in the present study, MMRP expression levels were classified as negative for $<10\%$ nuclear staining, and positive for $\geq10\%$ nuclear staining. Ki-67 was regarded as negative for $\leq40\%$ stained cells, and positive for $>40\%$ stained cells. Concerning EGFR, VEGF, and VEGFR2 expression, cases with score 0 were considered as negative while the remaining cases were considered as positive.

Statistical analyses

The Kolmogorov–Smirnov test was conducted to test that whether the quantitative values of this study followed a normal distribution. Continuous variables were expressed

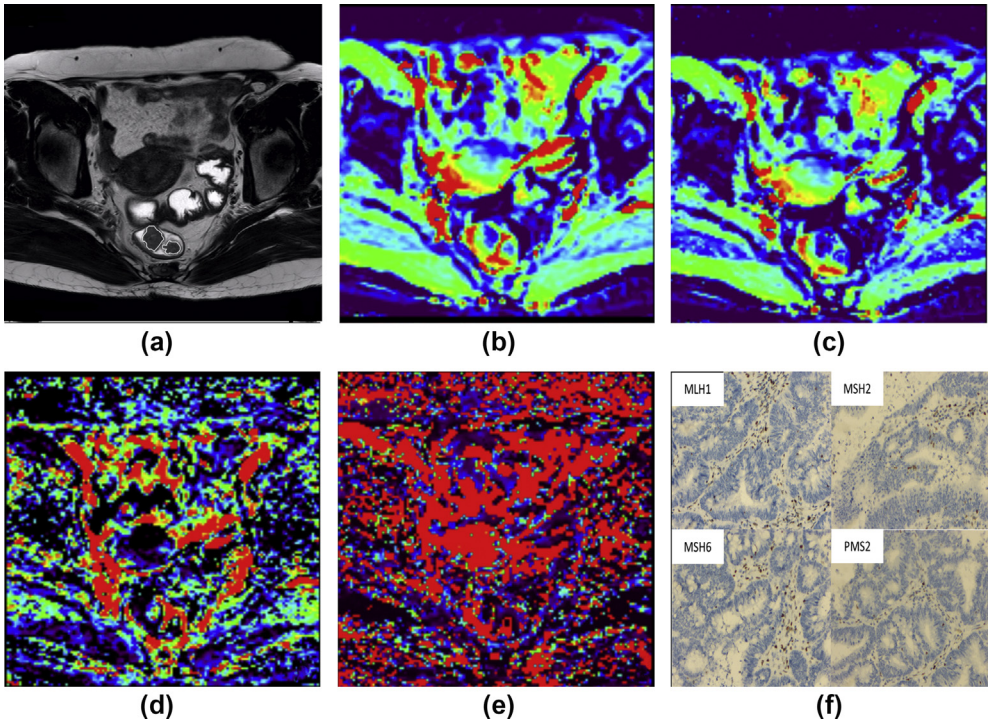

Figure 3 A 55-year-old woman with rectal cancer histopathologically diagnosed as stage T1 N0 cM0. (a) Axial T2-weighted MRI image shows two masses in the rectal wall. (b) The corresponding ADC, (c) pure diffusion coefficient D, (d) perfusion related fraction f; and (e) pseudo diffusion coefficient D* maps show that these two lesions have an average ADC value of 0.922×10^{-3} mm^2/s, a D value of 0.711×10^{-3} mm^2/s, a f value of 0.188 and a D* value of 17.392×10^{-3} mm^2/s, respectively. (f) Photomicrograph (Immunohistochemical staining, 200 ×) shows two adenocarcinomas with low expression levels of mismatch repair proteins (MMRP).

as the mean ± standard deviation. Analysis of those IVIM parameters between the two different MMRP expression levels of rectal cancers was performed using the Mann–Whitney U-test, as its distribution was skewed (confirmed by the Kolmogorov–Smirnov test). Receiver-operating characteristic (ROC) analysis was performed to evaluate the diagnostic performance of IVIM parameters in predicting MMRP expression levels preoperatively. The cut-off values with the largest Youden index [(sensitivity + specificity)−1] were calculated from the ROC curves. Ki-67, EGFR, VEGF, and VEGFR2 expression were compared between rectal cancers with different MMRP expression levels by the chi-square test. The interobserver agreement of IVIM parameters measurement was evaluated with intraclass correlation coefficient (ICC): poor (<0.50), moderate (0.50–0.75), good (0.75–0.90), and excellent (>0.90).[34] Statistical analysis was performed with SPSS 18.0 software (SPSS, Chicago, IL, USA). A value of $p<0.05$ was considered statistically significant.

Results

The IVIM values of rectal cancers with different MMRP expression levels are listed in Table 2. The f values of MMRP positive rectal cancers were significantly higher than negative cancers ($p=0.005$). The f values could differentiate MMRP-positive rectal cancers from negative cancers with an area under the curve (AUC) of 0.695 ($p=0.005$; Table 3, Fig 4). The VEGF and VEGFR2 expression rates of positive MMRP rectal cancers were significantly higher than those of negative MMRP cancers ($p=0.017$; Table 4). There was no difference in the expression of EGFR and Ki67 between MMRP-positive and -negative rectal cancers. Moreover, ADC and D values were not significantly different between the two groups of rectal cancers. Measurements of IVIM parameters in rectal cancers showed moderate intra- and interobserver agreement (ICC, 0.611–0.722; Table 5).

Discussion

IVIM MRI was successfully applied to evaluate rectal cancers with different MMRP expression levels. The DNA

Table 2
Intravoxel incoherent motion (IVIM) parameters of rectal cancers with different mismatch repair proteins (MMRP) expression levels.

IVIM parameter	MMRP (+)	MMRP (−)	*p*-Value
ADC	0.936±0.034	0.934±0.171	0.301
D	0.931±0.110	0.759±0.204	0.675
f	0.189±0.058	0.166±0.023	0.005[a]
D*	16.435±8.222	23.247±9.352	0.104

MMRP, mismatch repair proteins: negative, <10% nuclear staining; positive, ≥10% nuclear staining. The ADC, D and D* values are in units of $\times10^{-3}$ mm^2/s.
[a] $p<0.05$ with Mann–Whitney *U*-test.
ADC, apparent diffusion coefficient; D, pure diffusion coefficient; f, perfusion fraction; D*, pseudo-diffusion coefficient.

Table 3
Diagnostic performance of intravoxel incoherent motion parameters in distinguishing mismatch repair proteins (MMRP) positive rectal cancers from MMRP negative cancers.

Parameters	Cut-off	Sensitivity	Specificity	Accuracy	AUC	*p*-Value
ADC	0.997	18.8%	92.9%	65.6%	0.571	0.301
D	0.784	29.2%	92.9%	69.4%	0.529	0.675
f	0.183	52.1%	85.7%	73.3%	0.695	0.005[a]
D*	21.612	37.5%	89.3%	70.2%	0.612	0.104

The cut-off values of ADC, D and D* are in unit of $\times 10^{-3}$ mm^2/s.
[a]$p<0.05$ with ROC analysis.
ADC, apparent diffusion coefficient; D, pure diffusion coefficient; f, perfusion fraction; D*, pseudo-diffusion coefficient; AUC, area under the receiver operating characteristic (ROC) curve.

MMR system helps maintain genetic fidelity, and when defective, genetic errors accumulate, leading to colorectal tumorigenesis.[35,36]

In the current study, f values of MMRP-positive rectal cancers were significantly higher than negative cancers, which has not been reported previously. The f value corresponds to the vascular volume fraction of the tumour and represents tumour vascularisation to some extent,[37] which indicated that tumour vascularisation of MMRP-positive rectal cancers was higher than the negative cancers. The underlying mechanism might be involved in the signalling pathways of angiogenesis.

The present results showed that VEGF and VEGFR2 expression rates of positive MMRP rectal cancers were significantly higher than negative cancers. VEGF is considered as a potent angiogenic factor stimulator, and VEGF signalling pathways can regulate endothelial cell

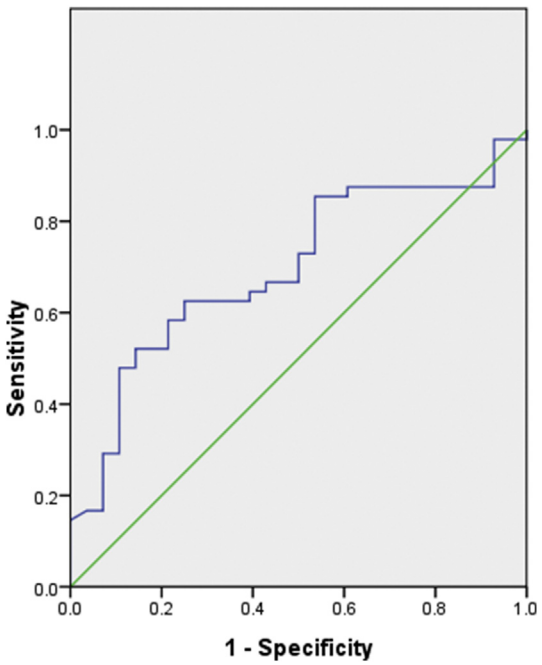

Figure 4 The ROC curve of the perfusion fraction (f) value in distinguishing MMRP positive rectal cancers from negative cancers (AUC=0.695, p=0.005). The reference line indicates random assignment.

Table 4
Association between mismatch repair proteins (MMRP) expression levels and histopathologic indexes.

		MMRP expression levels		*p*-Value
		Positive	Negative	
Ki-67	Positive	24	41	1.000
	Negative	4	7	
EGFR	Positive	10	16	0.834
	Negative	14	25	
VEGF	Positive	14	13	0.017‡
	Negative	7	25	
VEGFR2	Positive	14	13	0.017‡
	Negative	7	25	

[a]$p<0.05$ with chi-square test.
MMRP, mismatch repair proteins; EGFR, epidermal growth factor receptor; VEGF, vascular endothelial growth factor; VEGFR2, vascular endothelial growth factor receptor 2.

proliferation, migration, survival, and vascular permeability.[38] VEGFR2 is considered the most important angiogenesis-mediated receptor.[39] VEGF and VEGFR2 binding can stimulate tumour angiogenesis.[39] Angiogenesis permits rapid tumour growth and increases the potential for tumour metastasis.[40] Considering the significance of angiogenesis in tumorigenesis and metastatic processes, it is speculated that positive MMRP rectal cancers are more aggressive than negative cancers, and associated with worse prognosis, which is in accordance with previous studies.[41–44] Klau *et al.* reported that both histological parameter microvessel density (MVD) and microvessel area (MVA, the percentage of total tumour area occupied by vessels) can be used as histological parameters to characterise vascularisation of tumours and may therefore be used as surrogate markers for angiogenesis.[45] Given that MVD could be used as a surrogate marker for angiogenesis, there are several published reports in the literature that have investigated the correlation between IVIM-derived perfusion fraction (f) and MVD. Lee *et al.* found that IVIM-derived perfusion fraction (f) was positively correlated to MVD in a colorectal cancer mouse model.[46] This correlation has been demonstrated in human pancreatic tumour patients,[47] in VX2 liver tumours in rabbits,[48] in hepatocellular carcinomas in mouse xenograft tumour models,[49] in human gastric cancers mouse models,[50] and in nasopharyngeal carcinomas in nude mice[51]; however, there was no significant difference in the D* values between MMRP-positive and -negative rectal cancers. The perfusion-related fast

Table 5
Intra- and interobserver agreements for the measurements of intravoxel incoherent motion (IVIM) parameters in rectal cancers.

IVIM parameter	Intra-observer ICC (95% CI)	Interobserver ICC (95% CI)
ADC	0.901 (0.865–0.932)	0.785 (0.523–0.898)
D	0.912 (0.884–0.938)	0.793 (0.589–0.904)
F	0.883 (0.842–0.905)	0.693 (0.512–0.886)
D*	0.856 (0.838–0.886)	0.635 (0.503–0.818)

ADC, apparent diffusion coefficient; D, pure diffusion coefficient; f, perfusion fraction; D*, pseudo-diffusion coefficient; ICC, intraclass correlation coefficient; CI, confidential interval.

diffusion coefficient, D*, was more vulnerable to the signal-to-noise ratio and may have weak repeatability,[52] so required further confirmation.[53–55]

In the present study, there was no difference in the expression of epidermal growth factor receptor (EGFR) and Ki67 between MMRP-positive and -negative rectal cancers. The EGFR was the first identified member of the type I receptor tyrosine kinase family and is a major regulator of several distinct, diverse cellular pathways.[56] Activation of EGFR leads to downstream signalling, ultimately resulting in abnormal proliferation of cells.[57] Ki67 is a nuclear protein that is tightly linked to the cell cycle, and is considered to be a standard marker of tumour proliferation.[58,59] This may be attributed to the fact that EGFR and Ki67 are considered markers of proliferative activity in tumour cells, which was not significantly different between MMRP-positive and -negative rectal cancers. Moreover, ADC and D values were not significantly different between MMRP-positive rectal cancers and -negative cancers, which was similar to the results in endometrial carcinoma from the report of Minamiguchi *et al.*[60] The reason might be that ADC and D values reflected tumour cellularity and proliferation potential,[61–64] which was not significantly different between MMRP-positive and -negative rectal cancers.

The interobserver agreement was much less than intraobserver agreement, which may be attributed to the difference between the experience of the two observers. One observer had 7 years of experience in gastrointestinal radiology, and the other had 2 years of experience. The observer with 7 years of experience measured more accurately, but this did not affect the final measurement results.

Some limitations of the present study should be mentioned. First, it was a pilot study with a relatively small sample size independent of the authors' previous study,[30] which required more cases to confirm the findings. Second, ROIs were drawn manually without rigorous reference on postoperative specimens due to technique difficulty. Third, the diagnostic accuracy of f value in predicting MMR status of rectal cancers was relatively low, which required improvement in further study. Fourth, it is not known whether the immunohistochemical results could be applied to other cohorts, which was a defect of the present study and requires further investigation.

In conclusion, the f values derived from IVIM MRI differed significantly between rectal cancers with different MMRP expression levels, which might be indicative of different VEGF and VEGFR2 expression rates.

Conflict of interest

The authors of this manuscript declare no relationships with any companies whose products or services may be related to the subject matter of the article.

Acknowledgements

This work was supported by the National Natural Science Foundation of China (ID: 81671751, 81371516), Foundation of National Health and Family Planning Commission of China (W201306), Social Development Foundation of Jiangsu Province (BE2015605), Six Talent Peaks Project in Jiangsu Province (2015-WSN-079), Key Project and outstanding Youth supported by Medical Science and technology development Foundation Nanjing (YKK15067, QRX11178), Jiangsu province key medical young talents, "13th Five-Year" health promotion project of Jiangsu province (QNRC2016041).

References

1. Jemal A, Bray F, Center MM, *et al*. Global cancer statistics. *CA Cancer J Clin* 2011;**61**:69–90.
2. Nougaret S, Reinhold C, Mikhael HW, *et al*. The use of MR imaging in treatment planning for patients with rectal carcinoma: have you checked the "DISTANCE"? *Radiology* 2013;**268**:330–44.
3. Aaltonen LA, Peltomaki P, Leach FS, *et al*. Clues to the pathogenesis of familial colorectal cancer. *Science* 1993;**260**:812–6.
4. de Rosa N, Rodriguez-Bigas MA, Chang GJ, *et al*. DNA mismatch repair deficiency in rectal cancer: benchmarking its impact on prognosis, neoadjuvant response prediction, and clinical cancer genetics. *J Clin Oncol* 2016;**34**:3039–46.
5. Vasen HF, Blanco I, Aktan-Collan K, *et al*. Revised guidelines for the clinical management of Lynch syndrome (HNPCC): recommendations by a group of European experts. *Gut* 2013;**62**:812–23.
6. Bao F, Panarelli NC, Rennert H, *et al*. Neoadjuvant therapy induces loss of MSH6 expression in colorectal carcinoma. *Am J Surg Pathol* 2010;**34**:1798–804.
7. Radu OM, Nikiforova MN, Farkas LM, *et al*. Challenging cases encountered in colorectal cancer screening for Lynch syndrome reveal novel findings: nucleolar MSH6 staining and impact of prior chemoradiation therapy. *Hum Pathol* 2011;**42**:1247–58.
8. Bellizzi AM, Crowder CD, Marsh WL, *et al*. Mismatch repair status in a cohort of rectal adenocarcinomas before and after chemoradiation. *Mod Pathol* 2010;**23**:137A.
9. Shia J, Guillem JG, Moore HG, *et al*. Patterns of morphologic alteration in residual rectal carcinoma following preoperative chemoradiation and their association with long-term outcome. *Am J Surg Pathol* 2004;**28**:215–23.
10. Warrier SK, Trainer AH, Lynch AC, *et al*. Preoperative diagnosis of Lynch syndrome with DNA mismatch repair immunohistochemistry on a diagnostic biopsy. *Dis Colon Rectum* 2011;**54**:1480–7.
11. Kumarasinghe AP, de Boer B, Bateman AC, *et al*. DNA mismatch repair enzyme immunohistochemistry in colorectal cancer: a comparison of biopsy and resection material. *Pathology* 2010;**42**:414–20.
12. Shia J, Stadler Z, Weiser MR, *et al*. Immunohistochemical staining for DNA mismatch repair proteins in intestinal tract carcinoma: how reliable are biopsy samples? *Am J Surg Pathol* 2011;**35**:447–54.
13. Vilkin A, Halpern M, Morgenstern S, *et al*. How reliable is immunohistochemical staining for DNA mismatch repair proteins performed after neoadjuvant chemoradiation? *Hum Pathol* 2014;**45**:2029–36.
14. Rao SX, Zeng MS, Xu JM, *et al*. Assessment of T staging and mesorectal fascia status using high-resolution MRI in rectal cancer with rectal distention. *World J Gastroenterol* 2007;**13**:4141–6.
15. Giusti S, Buccianti P, Castagna M, *et al*. Preoperative rectal cancer staging with phased-array MR. *Radiat Oncol* 2012;**7**:29.
16. Ucar A, Obuz F, Sokmen S, *et al*. Efficacy of high resolution magnetic resonance imaging in preoperative local staging of rectal cancer. *Mol Imaging Radionucl Ther* 2013;**22**:42–8.
17. Jhaveri KS, Hosseini-Nik H. MRI of rectal cancer: an overview and update on recent advances. *AJR Am J Roentgenol* 2015;**205**:W42–55.
18. Le Bihan D, Breton E, Lallemand D, *et al*. MRI of intravoxel incoherent motions: application to diffusion and perfusion in neurologic disorders. *Radiology* 1986;**161**:401–7.
19. Sun Y, Tong T, Cai S, *et al*. Apparent diffusion coefficient (ADC) value: a potential imaging biomarker that reflects the biological features of rectal cancer. *PLoS One* 2014;**9**:e109371.
20. Curvo-Semedo L, Lambregts DM, Maas M, *et al*. Diffusion-weighted MRI in rectal cancer: apparent diffusion coefficient as a potential

noninvasive marker of tumor aggressiveness. *J Magn Reson Imaging* 2012;**35**:1365–71.
21. Akashi M, Nakahusa Y, Yakabe T, *et al*. Assessment of aggressiveness of rectal cancer using 3-T MRI: correlation between the apparent diffusion coefficient as a potential imaging biomarker and histologic prognostic factors. *Acta Radiol* 2014;**55**:524–31.
22. Le Bihan D, Breton E, Lallemand D, *et al*. Separation of diffusion and perfusion in intravoxel incoherent motion MR imaging. *Radiology* 1988;**168**:497–505.
23. Lu W, Jing H, Ju-Mei Z, *et al*. Intravoxel incoherent motion diffusion-weighted imaging for discriminating the pathological response to neoadjuvant chemoradiotherapy in locally advanced rectal cancer. *Sci Rep* 2017;**7**:8496.
24. Nougaret S, Vargas HA, Lakhman Y, *et al*. Intravoxel incoherent motion-derived histogram metrics for assessment of response after combined chemotherapy and radiation therapy in rectal cancer: initial experience and comparison between single-section and volumetric analyses. *Radiology* 2016;**280**:446–54.
25. Bäuerle T, Seyler L, Münter M, *et al*. Diffusion-weighted imaging in rectal carcinoma patients without and after chemoradiotherapy: a comparative study with histology. *Eur J Radiol* 2013;**82**:444–52.
26. Yu XP, Wen L, Hou J, *et al*. Discrimination between metastatic and nonmetastatic mesorectal lymph nodes in rectal cancer using intravoxel incoherent motion diffusion-weighted magnetic resonance imaging. *Acad Radiol* 2016;**23**:479–85.
27. Qiu L, Liu XL, Liu SR, *et al*. Role of quantitative intravoxel incoherent motion parameters in the preoperative diagnosis of nodal metastasis in patients with rectal carcinoma. *J Magn Reson Imaging* 2016;**44**:1031–9.
28. Bakke KM, Hole KH, Dueland S, *et al*. Diffusion-weighted magnetic resonance imaging of rectal cancer: tumour volume and perfusion fraction predict chemoradiotherapy response and survival. *Acta Oncol* 2017;**56**:813–8.
29. Surov A, Meyer HJ, Höhn AK, *et al*. Correlations between intravoxel incoherent motion (IVIM) parameters and histological findings in rectal cancer: preliminary results. *Oncotarget* 2017;**8**:21974–83.
30. Yan C, Pan X, Chen G, *et al*. A pilot study on correlations between preoperative intravoxel incoherent motion MR imaging and postoperative histopathological features of rectal cancers. *Transl Cancer Res* 2017;**6**:1050–60.
31. Kim HR, Kim HC, Yun HR, *et al*. An alternative pathway in colorectal carcinogenesis based on the mismatch repair system and p53 expression in Korean patients with sporadic colorectal cancer. *Ann Surg Oncol* 2013;**20**:4031–40.
32. Huh JW, Kim HC, Kim SH, *et al*. Mismatch repair gene expression as a predictor of tumor responses in patients with rectal cancer treated with preoperative chemoradiation. *Medicine (Baltimore)* 2016;**95**:e2582.
33. Jafarian AH, Kermani AT, Esmaeili J, *et al*. The role of COX-2 and Ki-67 overexpression in the prediction of pathologic response of rectal cancer to neoadjuvant chemoradiation therapy. *Indian J Cancer* 2016;**53**:548–51.
34. Vilar E, Gruber SB. Microsatellite instability in colorectal cancer: the stable evidence. *Nat Rev Clin Oncol* 2010;**7**:153–62.
35. Vilar E, Tabernero J. Molecular dissection of microsatellite instable colorectal cancer. *Cancer Discov* 2013;**3**:502–11.
36. Yuan SJ, Qiao TK, Qiang JW, *et al*. The value of DCE-MRI in assessing histopathological and molecular biological features in induced rat epithelial ovarian carcinomas. *J Ovarian Res* 2017;**10**:65.
37. Galizia G, Lieto E, Ferraraccio F, *et al*. Determination of molecular marker expression can predict clinical outcome in colon carcinomas. *Clin Cancer Res* 2004;**10**:3490–9.
38. Peng Y, Wang L, Du C, *et al*. Expression of vascular endothelial growth factor can predict distant metastasis and disease-free survival for clinical stage III rectal cancer following 30-Gy/10-f preoperative radiotherapy. *Int J Colorectal Dis* 2012;**27**:1555–60.
39. Koo TK, Li MY. A guideline of selecting and reporting intraclass correlation coefficients for reliability research. *J Chiropr Med* 2016;**15**:155–63.
40. Meng X, Li H, Kong L, *et al*. MRI in rectal cancer: correlations between MRI features and molecular markers Ki-67, HIF-1α, and VEGF. *J Magn Reson Imaging* 2016;**44**:594–600.
41. Popat S, Hubner R, Houlston RS. Systematic review of microsatellite instability and colorectal cancer prognosis. *J Clin Oncol* 2005;**23**:609–18.
42. Lanza G, Gafà R, Santini A, *et al*. Immunohistochemical test for MLH1 and MSH2 expression predicts clinical outcome in stage II and III colorectal cancer patients. *J Clin Oncol* 2006;**24**:2359–67.
43. Roth AD, Tejpar S, Delorenzi M, *et al*. Prognostic role of KRAS and BRAF in stage II and III resected colon cancer: results of the translational study on the PETACC-3, EORTC 40993, SAKK 60-00 trial. *J Clin Oncol* 2010;**28**:466–74.
44. Korphaisarn K, Pongpaibul A, Limwongse C, *et al*. Deficient DNA mismatch repair is associated with favorable prognosis in Thai patients with sporadic colorectal cancer. *World J Gastroenterol* 2015;**21**:926–34.
45. Klau M, Mayer P, Bergmann F, *et al*. Correlation of histological vessel characteristics and diffusion-weighted imaging intravoxel incoherent motion-derived parameters in pancreatic ductal adenocarcinomas and pancreatic neuroendocrine tumors. *Invest Radiol* 2015;**50**:792–7.
46. Lee HJ, Rha SY, Chung YE, *et al*. Tumor perfusion-related parameter of diffusion-weighted magnetic resonance imaging: correlation with histological microvessel density. *Magn Reson Med* 2014;**71**:1554–8.
47. Klau M, Mayer P, Bergmann F, *et al*. Correlation of histological vessel characteristics and diffusion-weighted imaging intravoxel incoherent motion-derived parameters in pancreatic ductal adenocarcinomas and pancreatic neuroendocrine tumors. *Invest Radiol* 2015;**50**:792–7.
48. Wu H, Liu H, Liang C, *et al*. Diffusion-weighted multiparametric MRI for monitoring longitudinal changes of parameters in rabbit VX2 liver tumors. *J Magn Reson Imaging* 2016;**44**:707–14.
49. Lee Y, Lee SS, Cheong H, *et al*. Intravoxel incoherent motion MRI for monitoring the therapeutic response of hepatocellular carcinoma to sorafenib treatment in mouse xenograft tumor models. *Acta Radiol* 2017;**58**:1045–53.
50. Song XL, Kang HK, Jeong GW, *et al*. Intravoxel incoherent motion diffusion-weighted imaging for monitoring chemotherapeutic efficacy in gastric cancer. *World J Gastroenterol* 2016;**22**:5520–31.
51. Cui Y, Zhang C, Li X, *et al*. Intravoxel incoherent motion diffusion-weighted magnetic resonance imaging for monitoring the early response to ZD6474 from nasopharyngeal carcinoma in nude mouse. *Sci Rep* 2015;**5**:16389.
52. Andreou A, Koh DM, Collins DJ, *et al*. Measurement reproducibility of perfusion fraction and pseudodiffusion coefficient derived by intravoxel incoherent motion diffusion-weighted MR imaging in normal liver and metastases. *Eur Radiol* 2013;**23**:428–34.
53. Qiu L, Liu XL, Liu SR, *et al*. Role of quantitative intravoxel incoherent motion parameters in the preoperative diagnosis of nodal metastasis in patients with rectal carcinoma. *J Magn Reson Imaging* 2016;**44**:1031–9.
54. Liu C, Wang K, Chan Q, *et al*. Intravoxel incoherent motion MR imaging for breast lesions: comparison and correlation with pharmacokinetic evaluation from dynamic contrast-enhanced MR imaging. *Eur Radiol* 2016;**26**:3888–98.
55. Zhang Q, Wang YX, Ma HT, *et al*. Cramer–Rao bound for intravoxel incoherent motion diffusion weighted imaging fitting. *Conf Proc IEEE Eng Med Biol Soc* 2013;**2013**:511–4.
56. Zwick E, Hackel PO, Prenzel N, *et al*. The EGF receptor as central transducer of heterologous signalling systems. *Trends Pharmacol Sci* 1999;**20**:408–12.
57. Yarden Y, Sliwkowski MX. Untangling the ErbB signalling network. *Nat Rev Mol Cell Biol* 2001;**2**:127–37.
58. Tan P-H, Bay B-H, Yip G, *et al*. Immunohistochemical detection of Ki67 in breast cancer correlates with transcriptional regulation of genes related to apoptosis and cell death. *Mod Pathol* 2005;**18**:374–81.
59. Fitzgibbons PL, Page DL, Weaver D, *et al*. Prognostic factors in breast cancer: college of American pathologists consensus statement 1999. *Arch Pathol Lab Med* 2000;**124**:966–78.
60. Minamiguchi K, Takahama J, Uchiyama T, *et al*. Uterine endometrial carcinoma with DNA mismatch repair deficiency: magnetic resonance imaging findings and clinical features. *Jpn J Radiol* 2018;**36**:429–36.
61. Fornasa F. Diffusion-weighted magnetic resonance imaging: what makes water run fast or slow? *J Clin Imaging Sci* 2011;**1**:27.
62. Driessen JP, Caldas-Magalhaes J, Janssen LM, *et al*. Diffusion-weighted MRI in laryngeal and hypopharyngeal carcinoma: association between apparent diffusion coefficient and histologic findings. *Radiology* 2014;**272**:456–63.
63. Heijmen L, ter Voert EEGW, Nagtegaal ID, *et al*. Diffusion-weighted MRI in liver metastases of colorectal cancer: reproducibility and biological validation. *Eur Radiol* 2013;**23**:748–56.
64. Surov A, Meyer HJ, Höhn AK, *et al*. Correlations between intravoxel incoherent motion (IVIM) parameters and histological findings in rectal cancer: preliminary results. *Oncotarget* 2017;**8**:21974–83.